

Accuracy requirements to test the applicability of the random cascade model to supersonic turbulence

Doris Folini¹ and Rolf Walder¹

École Normale Supérieure, Lyon, CRAL, UMR CNRS 5574, Université de Lyon, France
 e-mail: doris.folini@ens-lyon.fr

Received ... ; accepted ...

ABSTRACT

A model, which is widely used for inertial range statistics of supersonic turbulence in the context of molecular clouds and star formation, expresses (measurable) relative scaling exponents Z_p of two-point velocity statistics as a function of two parameters, β and Δ . The model relates them to the dimension D of the most dissipative structures, $D = 3 - \Delta/(1 - \beta)$. While this description has proved most successful for incompressible turbulence ($\beta = \Delta = 2/3$, and $D = 1$), its applicability in the highly compressible regime remains debated. For this regime, theoretical arguments suggest $D = 2$ and $\Delta = 2/3$, or $\Delta = 1$. Best estimates based on 3D periodic box simulations of supersonic isothermal turbulence yield $\Delta = 0.71$ and $D = 1.9$, with uncertainty ranges of $\Delta \in [0.67, 0.78]$ and $D \in [2.04, 1.60]$. With these 5-10% uncertainty ranges just marginally including the theoretical values of $\Delta = 2/3$ and $D = 2$, doubts remain whether the model indeed applies and, if it applies, for what values of β and Δ . We use a Monte Carlo approach to mimic actual simulation data and examine what factors are most relevant for the fit quality. We estimate that 0.1% (0.05%) accurate Z_p , with $p = 1, \dots, 5$, should allow for 2% (1%) accurate estimates of β and Δ in the highly compressible regime, but not in the mildly compressible regime. We argue that simulation-based Z_p with such accuracy are within reach of today's computer resources. If this kind of data does not allow for the expected high quality fit of β and Δ , then this may indicate the inapplicability of the model for the simulation data. In fact, other models than the one we examine here have been suggested.

Key words. Shock waves – Turbulence – Hydrodynamics – ISM:kinematics and dynamics – (Stars:) Gamma-ray burst: general – (Stars:) binaries (including multiple): close

1. Introduction

Supersonic turbulence is a key ingredient in various astrophysical contexts, from gamma ray bursts (Lazar et al. 2009; Narayan & Kumar 2009) or stellar accretion (Walder et al. 2008; Hobbs et al. 2011) to molecular clouds and star formation (Chabrier & Hennebelle 2011; Federrath & Klessen 2012; Padoan et al. 2012; Kritsuk et al. 2013). A key question is whether this turbulence, like incompressible turbulence, is characterized by universal statistics. Results from 3D periodic box simulations of driven, isothermal, supersonic turbulence (Kritsuk et al. 2007a; Schmidt et al. 2008; Pan et al. 2009) are indeed consistent with the highly compressible variant (Boldyrev 2002) of the hierarchical structure model that was put forward by She & Leveque (1994) for incompressible turbulence and that was further scrutinized by Dubrulle (1994) and She & Waymire (1995). This model is correspondingly popular in astrophysics. It is employed, for example, in the interpretation of molecular cloud observations (Gustafsson et al. 2006; Hily-Blant et al. 2008) or to derive a theoretical expression for the density distribution in supersonic turbulence (Boldyrev et al. 2002), which enters theories of the stellar initial mass function (Hennebelle & Chabrier 2008).

Nevertheless, some doubts remain whether the model really applies to simulation data of supersonic turbulence and, if so, with what parameter values. The best-fit model parameters that we are aware of (Pan et al. 2009) still come with a 5-10% uncertainty range that is only marginally compatible with theoretically predicted parameter values (see below). Here we argue that

today's computer resources should allow for 1-2% accurate parameter fits in the highly compressible regime, thereby likely settling the issue. Our claim is based on a Monte Carlo approach to mimic actual simulation data.

The hierarchical structure model predicts the ratios Z_p of (observable) structure function scaling exponents ζ_p , $p = 1, 2, 3, \dots$ etc., of a 3D velocity field \mathbf{u} as

$$Z_p = \frac{\zeta_p}{\zeta_3} = (1 - \Delta)\frac{p}{3} + \frac{\Delta}{1 - \beta} (1 - \beta^{p/3}). \quad (1)$$

Here, $D = 3 - C$ is the dimension of the most intermittent structure, $C = \Delta/(1 - \beta)$ the associated co-dimension, $\beta \in [0, 1]$ measures the intermittency of the energy cascade, and $\Delta \in [0, 1]$ measures the divergent scale dependence of the most intermittent structures. The ζ_p are defined in the inertial range by

$$S_p(r) \equiv \langle |\mathbf{u}(\mathbf{x} + \mathbf{r}) - \mathbf{u}(\mathbf{x})|^p \rangle \propto r^{\zeta_p}, \quad (2)$$

where $\langle \dots \rangle$ denotes the average over all positions \mathbf{x} within the sample and over all directed distances \mathbf{r} . The Z_p should be well defined over a larger range because of extended self-similarity (Benzi et al. 1993) and Eq. 1 should remain formally valid for generalized structure functions $\tilde{S}_p(r)$, computed from mass-weighted velocities $\mathbf{v} \equiv \rho^{1/3}\mathbf{u}$ (Kritsuk et al. 2007a,b).

Several special cases of the model that differ in their parameter values exist in the literature (see e.g. the review by She & Zhang 2009). The original model by She & Leveque (1994) applies most successfully to incompressible turbulence with 1D vortex filaments as most dissipative structures ($D = 1$)

arXiv:1602.02121v1 [astro-ph.CO] 4 Feb 2016

and parameter values $\beta = \Delta = 2/3$. For highly compressible turbulence, parameter values remain debated. Boldyrev (2002) argues that the most dissipative structures are 2D shocks, thus $D = 2$, and chose to keep $\Delta = 2/3$ and set $\beta = 1/3$. By contrast, Schmidt et al. (2008) argue that $\Delta = 1$ (implying $\beta = 0$) to be consistent with Burgers turbulence. A few studies used 3D simulation data, derived sets of Z_p , and attempted simultaneous fits of β and Δ (Kritsuk et al. 2007b; Schmidt et al. 2008, 2009; Folini et al. 2014). The results are inconclusive in that fits of similar quality are obtained for widely different β - Δ -pairs. Also using 3D simulation data (1024^3 , Mach 6) but working with density-weighted moments of the dissipation rate, Pan et al. (2009) simultaneously fitted Δ and D to their data. They find $\Delta \in [0.67, 0.78]$ and $D \in [2.04, 1.60]$, with a best estimate of $\Delta = 0.71$ and $D = 1.9$, thus $\beta = 0.35$. The range for Δ is not compatible with the suggested $\Delta = 1$ (see above), and also $\Delta = 2/3$ lies only at the lower-most bound of the inferred range. Both Δ and β may thus deviate from their incompressible values ($\beta = \Delta = 2/3$) as the Mach number increases, making simultaneous determination of β and Δ a must.

The present study is motivated by this still inconclusive situation. We want to better understand what factors (accuracy / order of Z_p ; mildly versus highly compressible turbulence) are most relevant for the fit quality and why widely different β - Δ -pairs yield fits of similar quality. We use this insight to formulate quantitative estimates of what is needed to obtain 1% accurate estimates of β and Δ . We present results in Sect. 2, discuss them in Sect. 3, and conclude in Sect. 4.

2. Results

We first show that β and Δ can be uniquely determined from an associated (i.e. computed via Eq. 1) pair Z_{p_1} and Z_{p_2} . We then illustrate how uncertainties in Z_p map onto the β - Δ -plane. Finally, we give estimates on how accurate the Z_p have to be to achieve a desired accuracy of β , Δ , and C .

2.1. β and Δ from exact Z_p

Consider two values Z_{p_1} and Z_{p_2} that both fulfill Eq. 1 for the same values (β, Δ). In the following, we show that (β, Δ) can unambiguously (uniquely) be recovered from Z_{p_1} and Z_{p_2} .

We start by rewriting Eq. 1, factoring out Δ :

$$0 = \Delta \left(\frac{3(1 - \beta^{p/3}) - p(1 - \beta)}{3(1 - \beta)} \right) + \left(\frac{p - 3Z_{p_i}}{3} \right), \quad j = 1, 2. \quad (3)$$

Using Z_{p_1} , we can obtain an expression for Δ ,

$$\Delta = \left(\frac{3Z_{p_1} - p_1}{3} \right) \left(\frac{3(1 - \beta)}{3(1 - \beta^{p_1/3}) - p_1(1 - \beta)} \right). \quad (4)$$

By now writing Eq. 3 with $Z_p = Z_{p_2}$, using Eq. 4 to replace Δ , do some re-ordering of terms, and abbreviating $p_1/3 \equiv a$ and $p_2/3 \equiv b$, we end up with the following equation for β :

$$0 = \left(\frac{-\beta^b + b\beta + 1 - b}{-\beta^a + a\beta + 1 - a} \right) - \left(\frac{Z_{p_2} - b}{Z_{p_1} - a} \right) \equiv \frac{P_{\beta,b}}{P_{\beta,a}} - R_{a,b}, \quad (5)$$

or

$$R_{a,b} P_{\beta,a} = P_{\beta,b}. \quad (6)$$

The polynomial $P_{\beta,x} \equiv -\beta^x + x\beta + 1 - x$, with $x > 0$ and $\beta \in (0, 1)$, is a monotonically decreasing (increasing) function for $x < 1$

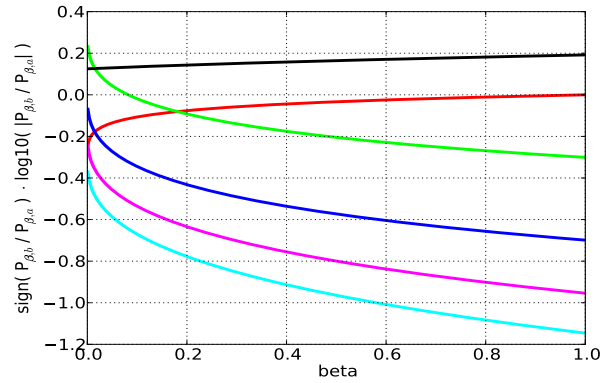


Fig. 1. Ratio of polynomials $P_{\beta,b}/P_{\beta,a}$, Eq. 5, (y-axis, shown as logarithm) for selected exponents a and b as function of β (x-axis). Colors indicate $b/a = 2$ (red), 4 (green), 5 (blue), 6 (magenta), 7 (cyan), all with $a = p_1/3 = 1/3$, as well as $b/a = 7/6$ (black) with $a = p_1/3 = 6/3$.

($x > 1$), as can be seen by taking the derivative of $P_{\beta,x}$ with respect to β and as illustrated in Fig. 1. Consequently, Eq. 6 has a unique solution, β , from which Δ can be recovered via Eq. 4. Thus Eq. 1 defines an exact one-to-one correspondence between pairs (Z_{p_1}, Z_{p_2}) and (β, Δ) .

Two more points deserve to be highlighted, with the help of Fig. 1. The ratio $P_{\beta,b}/P_{\beta,a} = R_{a,b}$ is shown as a function of β for different a and b or, equivalently, p_1 and p_2 . From the figure it can be taken that, first, largely different values of p_1 and p_2 are advantageous since they result in stronger stratification of β with respect to $R_{a,b} = (Z_{p_2} - b)/(Z_{p_1} - a)$. The cyan curve in Fig. 1, which represents $p_1/p_2 = 1/7$, covers a wider range of values on the y-axis than the black curve ($p_1/p_2 = 6/7$). Secondly, the stratification is stronger for small β . Somewhat anticipating Sect. 2.2, we thus expect uncertainties in the Z_p to be less important if Z_p are available for largely different p and if they are associated with (yet to be determined) small values of β .

2.2. Uncertainty of Z_p in the β - Δ -plane

2.2.1. Single Z_p

From Eq. 4 it is clear that each Z_p defines a curve in the β - Δ -plane. If Z_p is derived from model data or observations, it will typically come with an uncertainty estimate, e.g. $\delta Z_p/Z_p \leq 5\%$, with δ indicating the uncertainty. In the β - Δ -plane, this uncertainty range translates into an area around the Z_p curve. An illustration is given in Fig. 2. The following points may be made.

One value of Z_p (a line of constant Z_p in the β - Δ -plane) is compatible with a (large) range of β and / or Δ that always includes $\Delta = 1$ and $\beta = 0$. The range tends to be smaller for Z_p associated with small β and large Δ (i.e. the lower right corner of β - Δ -plane). Uncertainties associated with Z_p (5% in Fig. 2, white curves) augment the range, especially for $p = 2$ and $p = 4$, as well as for small Δ and large β (top left corner of the plane). Also apparent from Fig. 2 (or from taking the derivative with respect to Δ of Eq. 1): for fixed β and $p < 3$ ($p > 3$), Z_p is a monotonically increasing (decreasing) function of Δ . A similar statement holds for Z_p as a function of β for fixed Δ .

In summary, we expect uncertainties in the Z_p to be more of an issue if only low orders of p (up to about 4) are available and / or if the (yet to be determined) β is large.

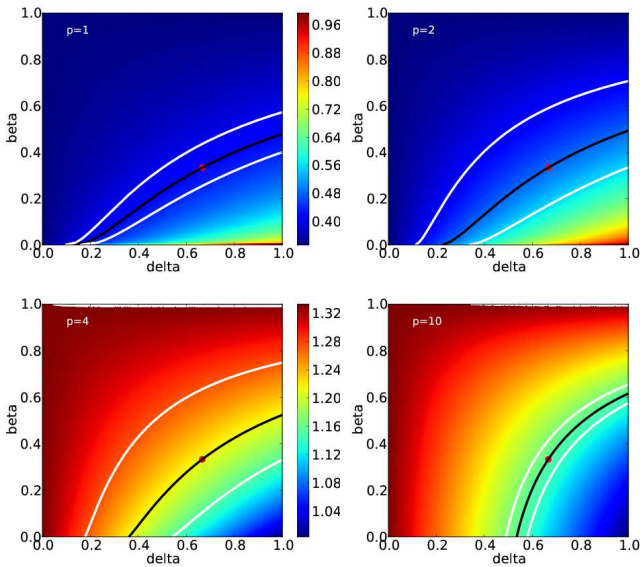


Fig. 2. Z_p in the β - Δ -plane, role of p . Shown is Z_p (color coded) for $p = 1$ (top left), $p = 2$ (top right), $p = 4$ (bottom left) and $p = 10$ (bottom right). For $\beta = 1/3$ and $\Delta = 2/3$ (red dot), the curve of constant Z_p (black) is shown, as well as curves of $\pm 5\%$ different Z_p (white).

2.2.2. Multiple Z_p

We now turn to multiple Z_p and their associated uncertainty ranges δZ_p , and ask what area they define in the β - Δ -plane. An illustration is given in Fig. 3. Starting from one specific pair of $\beta = 1/3$ and $\Delta = 2/3$ and computing Z_p for $p = 1, \dots, 5$ (left) or $p = 1, \dots, 7$ (right), we show pairs of 5% perturbed Z_p curves, i.e. $1.05 \cdot Z_p$ and $0.95 \cdot Z_p$.

As can be seen, only a small fraction of the β - Δ -plane lies between all pairs of perturbed curves. Yet this area comprises a wide range of (β, Δ) values or co-dimensions. The 5% uncertainty in the Z_p translates into a much larger uncertainty (in percent) for β and Δ . Closer inspection reveals that the area is actually defined by only two sets of curves: those for $p = 1$ and $p = 5$ (left panel) or $p = 7$ (right panel). The latter area is smaller, which indicates that higher order structure functions constrain the problem of finding β and Δ from a set of Z_p more strongly. Also apparent from Fig. 3 is the dominant role of the $p = 1$ curve for narrowing down the composite area between all curves. All this is in line with the expectation (see Sects. 2.1) that Z_p for largely different p are advantageous for the determination of β and Δ .

The relevance of the overall location in the β - Δ -plane is illustrated in Fig. 4. Again, the area shown is contained within 5% perturbed Z_p curves for two additional (β, Δ) pairs. As can be seen, smaller values of β (lower panels) result in smaller areas, independent of Δ . The crucial role of the $p = 1$ (white) and $p = 5$ (green) curves for confining the area persists. Table 1 gives a quantitative idea of the relevance of β , Δ , δZ_p , and p_{\max} for the uncertainty range $\pm \delta C$ of the co-dimensions C . A small δC basically requires a small δZ_p , a large p_{\max} , a small β , and a large Δ . The concrete numbers highlight the difficulty (or ill-posedness) of the problem. The situation is worse for larger β (bottom rows in Table 1) and better for smaller values of β (not shown).

We emphasize that the above considerations serve only as illustration. We looked at the area confined by a set of $Z_p \pm \delta Z_p$ curves. We have not yet considered the problem of estimating

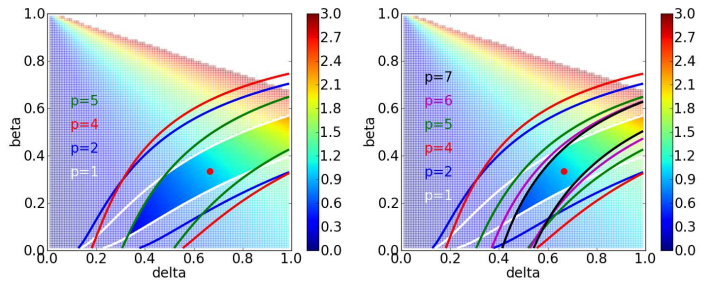


Fig. 3. Part of β - Δ -plane (color coded in co-dimension $C = \Delta/(1 - \beta)$, $0 < C < 3$) within joint reach of (at most) 5% perturbed Z_p , starting from Z_p for $\Delta = 2/3$ and $\beta = 1/3$ (red dot). Left panel: Curves of 5% perturbed Z_p values for $p = 1$ (white), $p = 2$ (blue), $p = 4$ (red), and $p = 5$ (green) and part of the β - Δ -plane enclosed by all of them. Right panel: Same as left panel but also including $p = 6$ (purple) and $p = 7$ (black).

best-fit β_f , Δ_f , and thus C_f for a set of given Z_p . Such a best-fit solution may lie outside the area considered here.

In summary, very accurate Z_p are needed to derive reliable best estimates for β , Δ , and C , and smaller values of β help.

2.3. Best-fit β_f and Δ_f from uncertain Z_p

We now turn to our actual problem of interest: given a set of perturbed (uncertain) $\tilde{Z}_p = Z_p + \delta Z_p$, what are associated best-fit estimates for β_f and Δ_f ? Different techniques exist to cope with this kind of question (e.g. Najm 2009; Le Maître & Knio 2010). We use a simple Monte Carlo approach.

We start with a pair (β, Δ) and a maximum order p_{\max} , then use Eq. 1 to obtain a set of $Z_p = Z_p(\beta, \Delta)$ for $p = 1$ to $p = p_{\max}$. Each of these Z_p we perturb randomly (uniformly distributed random numbers) by, at most, $\alpha\%$, which gives us a perturbed set of \tilde{Z}_p . For this set of \tilde{Z}_p we then seek to find best-fit β_f and Δ_f . In the following, we do not consider one set of \tilde{Z}_p , as would be the case in a real application (unless multiple time slices are available, see Sect. 3). Instead, we take a statistical view for the problem by looking at a large number (1000 to 100 000, see below) of randomly generated sets of perturbed \tilde{Z}_p . This enables us, in a statistical sense, to relate the accuracy of the \tilde{Z}_p with the accuracy of the fitted parameters. Our approach leaves us with two free parameters, the uncertainty α and the maximum order p_{\max} .

2.3.1. Minimization of least square error in Z_p

A straightforward way to determine best-fit β_f and Δ_f for any given set of \tilde{Z}_p , $p = p_{\min} \dots p_{\max}$ is to minimize

$$\sum_{p=1}^{p_{\max}} [\tilde{Z}_p - Z_p(\beta_f, \Delta_f)]^2 \quad (7)$$

over the β - Δ -plane. To find the minimum, we compare the \tilde{Z}_p with pre-computed values $Z_p(\beta, \Delta)$ on a fine β - Δ -grid ($\beta, \Delta \in (0, 1)$; grid-spacing 0.002). The associated co-dimension is given by $C_f = \Delta_f/(1 - \beta_f)$.

To capture the range of potential outcomes for a range of similarly perturbed data sets \tilde{Z}_p , we produced 100 000 perturbed data sets, for each of which we determined β_f and Δ_f . For initial values $(\beta, \Delta) = (1/3, 2/3)$ and (at most) 5% perturbed Z_p for $p = 1, \dots, 5$, the result is summarized in Fig. 5.

Table 1. Illustration of range δC of co-dimension C for given order p and uncertainty δZ_p of structure functions for two β - Δ pairs.

$\beta = 1/3, \Delta = 2/3, C = 1$			
$\delta Z_p/Z_p = 1\%$	$p = 1, \dots, 9$		
$p = 1, \dots, 5:$	0.79 – 1.46	$\delta Z_p/Z_p = 1\%:$	0.93 – 1.08
$p = 1, \dots, 6:$	0.83 – 1.23	$\delta Z_p/Z_p = 2\%:$	0.84 – 1.27
$p = 1, \dots, 7:$	0.87 – 1.18	$\delta Z_p/Z_p = 3\%:$	0.74 – 1.52
$p = 1, \dots, 8:$	0.90 – 1.13	$\delta Z_p/Z_p = 4\%:$	0.70 – 1.92
$p = 1, \dots, 9:$	0.93 – 1.08	$\delta Z_p/Z_p = 5\%:$	0.65 – 2.25
$\beta = 2/3, \Delta = 2/3, C = 2$			
$\delta Z_p/Z_p = 1\%$	$p = 1, \dots, 9$		
$p = 1, \dots, 5:$	0.51 – 3.00	$\delta Z_p/Z_p = 1\%:$	1.11 – 3.00
$p = 1, \dots, 6:$	0.70 – 3.00	$\delta Z_p/Z_p = 2\%:$	0.71 – 3.00
$p = 1, \dots, 7:$	0.86 – 3.00	$\delta Z_p/Z_p = 3\%:$	0.55 – 3.00
$p = 1, \dots, 8:$	1.00 – 3.00	$\delta Z_p/Z_p = 4\%:$	0.44 – 3.00
$p = 1, \dots, 9:$	1.11 – 3.00	$\delta Z_p/Z_p = 5\%:$	0.36 – 3.00

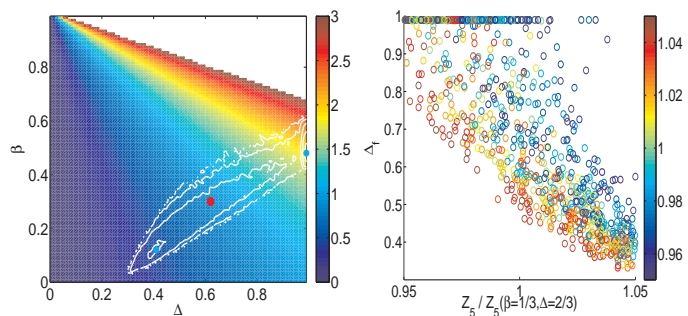


Fig. 5. Best-fit β_f and Δ_f from 5% perturbed Z_p . Left: 2D histogram (contours, log10, spacing 0.5, spanning three orders of magnitude) of best-fit β - Δ -values from 100 000 perturbed data sets. We note that the 2D histogram shows two peak values (indicated by cyan dots), none of them co-located with the unperturbed ($\beta = 1/3, \Delta = 2/3$) pair (red dot). Right: Underestimation of Z_5 favors $\Delta_f = 1$. Shown is, for a subset of 1000 perturbed data sets, Δ_f as function of \tilde{Z}_5/Z_5 , again for an unperturbed pair ($\beta = 1/3, \Delta = 2/3$). Colors indicate \tilde{Z}_1/Z_1 .

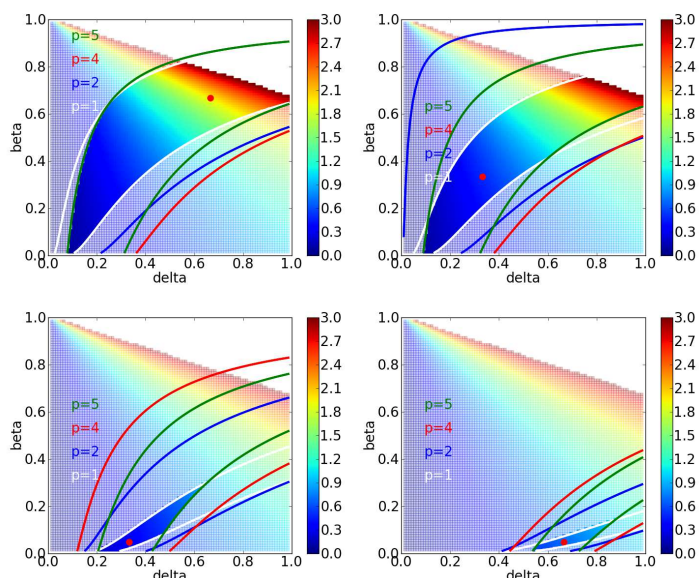


Fig. 4. Same as Fig. 3, left, but for $\beta = \Delta = 2/3$ (top left), $\beta = \Delta = 1/3$ (top right), $\beta = 0.048$ and $\Delta = 1/3$ (bottom left), as well as $\beta = 0.048$ and $\Delta = 2/3$ (bottom right).

Shown in the left panel of Fig. 5 is a 2D histogram (contours) of our 100 000 best-fit (β_f, Δ_f) pairs. Two points are noteworthy. First, the overall area defined by the histogram is similar to the area in Fig. 3, left panel. This is remarkable since the area in Fig. 3 is strictly defined by the 5% uncertainty of the Z_p , whereas the area in Fig. 5 is defined through a minimization problem. Second, the 2D histogram has an interior structure with two peaks, around $(\beta, \Delta) = (0.1, 0.4)$ or $C = 0.4$ and $(\beta, \Delta) = (0.45, 1.0)$ or $C = 1.8$ (cyan dots). None of them is co-located with the initial, unperturbed $(\beta, \Delta) = (1/3, 2/3)$ pair (red dot, $C = 1$).

Three questions come to mind. Where do the two peaks in the 2D histogram come from? Do other (β, Δ) pairs result in a qualitatively different picture? Can the minimization procedure be improved to better recover the initial, unperturbed (β, Δ) pair? We address the first two questions in the following while postponing the third question for Sect. 2.3.2.

The existence and location of the two peaks can be understood, at least qualitatively, from two observations. First, minimization via Eq. 7 gives more weight to larger p , as they are associated with larger values of Z_p . Roughly speaking, the best-fit (β_f, Δ_f) pair tends to lie on or close to the curve defined by \tilde{Z}_5 . Moving away from that curve results in a large penalty in the form of a large contribution to the sum in Eq. 7. Second, this translates the minimization problem into the question of where the curves for $p < 5$ come closest to the curve defined by \tilde{Z}_5 . For illustration, we consider two extreme values of \tilde{Z}_5 . To stay on the lower green curve in the left panel of Fig. 3, ($\tilde{Z}_5 = 0.95Z_5$) and, at the same time, be as close as possible to any of the white curves ($p = 1$) results in a (β_f, Δ_f) pair to the right, at $\Delta_f = 1$. By contrast, the upper green curve (105% of the exact Z_5 curve) only comes closest to (intersects) any white curve between 95% Z_1 and 105% Z_1 in a region further to the left. Clearly, the full problem is more intricate, with also curves for Z_2 and Z_4 , and the Z_5 curve not necessarily adopting one of its two extreme values. Nevertheless, Fig. 5, right panel, suggests the full data to be in line with the above reasoning. For 1000 randomly picked data sets from the left panel, we show Δ_f as a function of \tilde{Z}_5/Z_5 , with Z_5 the exact value. Colors indicate \tilde{Z}_1/Z_1 . As can be seen, $\Delta_f = 1$ indeed tends to be associated with small \tilde{Z}_5 and small \tilde{Z}_1 (lower green and upper white curve in Fig. 3, left panel). Particularly low values of Δ_f (e.g. $\Delta_f \approx 0.4$) tend to occur for large \tilde{Z}_5 and any \tilde{Z}_1 (upper green curve and any white curve in Fig. 3, left panel).

Concerning other initial values (other exact (β, Δ) pairs), a similar situation arises in the sense that double peaked histograms emerge. Details depend, however, on the concrete values of β and Δ , on the assumed uncertainty (5% or more / less), and on p_{\max} . An illustration is given in Fig. 6, by means of 1D histograms of $C_f = \Delta_f/(1 - \beta_f)$. These 1D histograms are less intricate than the 2D histogram in Fig. 5, left, yet still capture the essentials. We show histograms for $\Delta = 2/3$ and different values of $\beta \in [0.0476, 2/3]$ (corresponding to $C \in [0.7, 2]$) and accuracies between 0.1% and 20%. Five points may be made. First, the double-peaked structure that is apparent in the β - Δ plane in Fig. 5 re-appears as a double peak in the 1D C_f -histograms of Fig. 6 (panel in row three, column three). Second, the double-peak vanishes as β and the uncertainty both become small (lower left corner of the figure). For the same uncertainty, the double-peak exists for large β but not for small β (third row in Fig. 6).

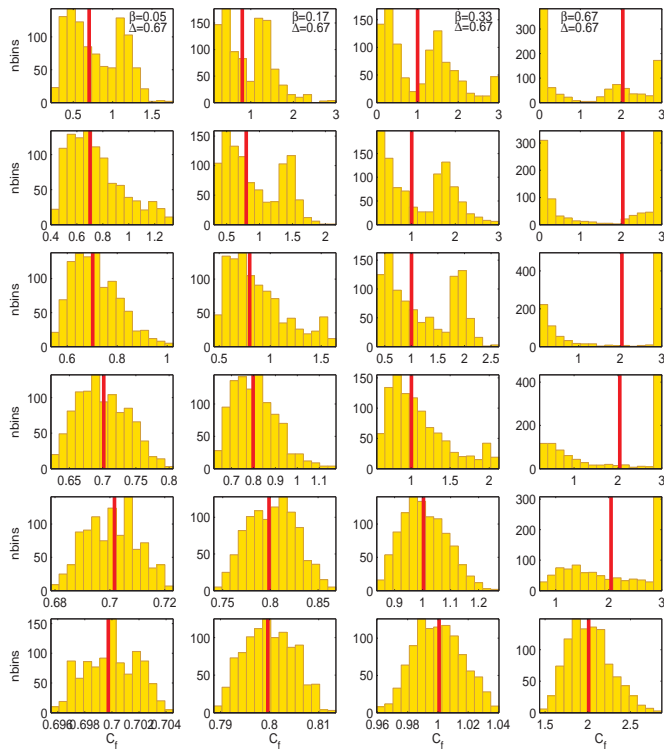


Fig. 6. Role of β (columns) and accuracy (rows) of associated Z_p , for fixed $\Delta = 2/3$. Shown are PDFs (y-axis) of C_f (x-axis), 1000 random data sets, powers $p = 1, \dots, 5$ for $\beta=0.0476$ (first column), $\beta=0.17$ (second column), $\beta=1/3$ (third column), and $\beta = 2/3$ (fourth column). Corresponding exact co-dimensions (red lines) are, from left to right: $C = 0.7$, $C = 0.8$, $C = 1$, and $C = 2$. Individual rows from top to bottom contain accuracies of 20%, 10%, 5%, 2%, 0.5%, and 0.1%. As can be seen, the larger β , the more severe are the consequences of inaccuracies in the Z_p . Histograms in the upper right (large β , low accuracy of the Z_p) look worst. We note that axis ranges differ among panels, to best capture the shape of each histogram.

For the same β , the double-peak exists for large uncertainties but not for small ones (second column of Fig. 6). Third, going to really small values of β and the uncertainty, the histogram becomes symmetric with one central peak. Fourth, only for these really small values is the co-dimension of the initially prescribed (β, Δ) pair (shown in red) co-located with the peak of the histogram. Fifth, for $\beta = \Delta = 2/3$ (right column) the histogram peaks at $C_f = 3$ instead of $C = 2$, unless the accuracy is really high (0.1%, last row). This is understandable from the arguments presented above, with regards to the origin of the two peaks in the 2D histogram in Fig. 5, and from looking at the green ($p = 5$) and white ($p = 1$) curves in Fig. 4, upper left panel.

In summary, unless both, δZ_p and β are small, best-fit values will preferentially reside in either one of the two peaks of the histograms in Figs. 5 or 6 instead of merely scattering around the correct solution, as in Fig. 6, lower left panel.

2.3.2. Alternative ways to obtain best-fit β_f and Δ_f

A number of ideas come to mind on how one may improve the best-fit approach detailed in Sect. 2.3.1.

Recalling the findings in Sect. 2.2.1, including higher values of p in the best-fit estimate should improve the situation. From Fig. 7 it can be taken that this is indeed the case, at least for the example shown ($\beta = 1/3$, $\Delta = 2/3$, accuracy of 5%). However,

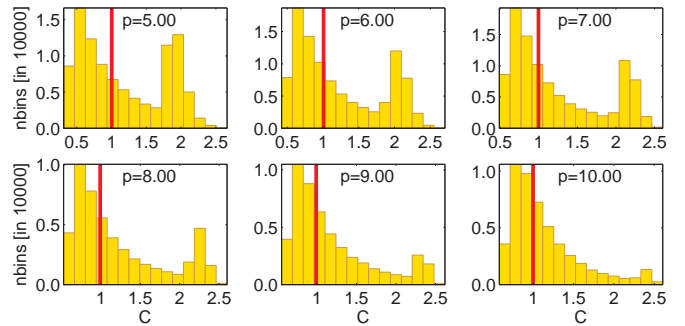


Fig. 7. Role of higher order moments. Inclusion of higher order ESS scaling exponents (from $p = 5$, top left, to $p = 10$, bottom right) gradually reduces the erroneous peak in the best-fit co-dimension (around $C_f = 2.5$). Shown are PDFs of C_f for at most 5% perturbed Z_p values (100 000 random data sets) and exact pair ($\beta = 1/3$, $\Delta = 2/3$). Spacing of the β - Δ -grid for fitting is 0.002.

the improvement may be regarded as rather modest. Going from $p = 5$ to $p = 10$, as is illustrated in the figure, has about the same effect as staying with $p = 5$ but going from an accuracy of 5% to an accuracy of 2%. From a practical point of view it also seems questionable whether high order structure functions can meet the accuracy requirements. In numerical simulations, higher order structure functions are probably more prone to the bottleneck effect (Dobler et al. 2003; Kritsuk et al. 2007a).

Another way to improve the situation could be to go to weighted root mean squares instead of the unweighted sum in Eq. 7. Hopefully this breaks the dominant role of the highest order Z_p available (see Sect. 2.3.1) and, ultimately, leads to more accurate best-fit β_f and Δ_f . Two weightings come to mind. On the one hand, weights proportional to the inverse of the Z_p with the goal of giving equal weight to each term in the sum, thus reducing the "overweight" of larger p in the sum. On the other hand, we could try to give more weight to p terms with a higher accuracy (smaller δZ_p). Corresponding information may be available, e.g. from the numerical determination of the Z_p . We tried both ideas but neither choice of weights decidedly improved the best-fit values. Weighting tends to change the relative height of the two peaks in the double peaked histograms of Fig. 6, but it does not get rid of the double peaked structure.

We interpret this finding in the following way. First, there are likely always several Z_p that do not have their exact values and thus draw the solution in different directions, away from its exact value. Second, the different curve shapes are important so that, even for weighted sums, the terms $p = 1$ and $p = p_{\max}$ are of crucial importance for the overall fit.

In summary, none of the above alternative ways of fitting simultaneously for β and Δ provides clearly superior results to what can be obtained from the straightforward minimization of Eq. 7. We conclude that, for successful two-parameter fits of β and Δ , highly accurate Z_p are a must. A quantitative estimate of "highly accurate" is given in the next section.

2.3.3. Required accuracy of Z_p for 'good' best-fit β_f and Δ_f

We now ask how accurate the Z_p have to be in order to reach a prescribed accuracy of $C_f = \Delta_f / (1 - \beta_f)$ via fitting β_f and Δ_f .

We formulate our accuracy goal in terms of only C_f , since we illustrated in Sect. 2.3.1 that a single peaked and roughly symmetric distribution of C_f goes hand in hand with high accuracy, not only of C_f but also of the underlying two parameter fit, β_f and Δ_f . If the latter is not accurate enough, a double peaked dis-

tribution for C_f results. We find, as a rule of thumb, a single peak distribution if $2/3$ of all C_f lie within 10% or better of the exact C . We use Eq. 7 for the two parameter fit, as the more elaborate attempts of Sect. 2.3.2 gave no decidedly better results. As theoretical arguments suggest $\Delta = 2/3$ or larger (Dubrulle 1994; Schmidt et al. 2008), we concentrate on that part of the β - Δ -plane.

In practical terms, we define a grid of exact pairs (β, Δ) via a (nearly) equidistant grid of $C = 0.4, \dots, 2$ and $\Delta = 0.7, \dots, 0.99$ plus, in addition, $\Delta = 2/3$. We equally define some fixed levels of perturbations: $\delta Z_p/Z_p$ (in %) $\in [0.05, 0.1, 0.2, 0.5, 1, 2, 5, 10, 15, 20]$. For each exact pair and each perturbation, we created 1000 perturbed sets of \tilde{Z}_p , $p = 1, \dots, 5$ (see Sect. 2.3). Each perturbed set is fitted via Eq. 7. For each initial pair (β, Δ) and for each prescribed $\delta Z_p/Z_p$ this yields 1000 fitted pairs (β_f, Δ_f) and derived co-dimensions C_f . These can, in principle, be arranged in histograms, as in Fig. 6. Finally, we identify the largest $\delta Z_p/Z_p$ for which $2/3$ of all C_f lie within the demanded accuracy of the exact, initial C .

Fig. 8 illustrates the result. Obviously, the accuracy of the \tilde{Z}_p (colored squares, in %) that is needed to get at least $2/3$ of best-fit C_f to lie within 10% (top panel) or 5% (bottom panel) of the exact (initial) C depends on the position within the β - Δ -plane. In the lower right parts, $\delta Z_p/Z_p \geq 1\%$ is sufficient to get 10% accurate C_f , and $\delta Z_p/Z_p \geq 0.5\%$ yields 5% accurate C_f . By contrast, in the upper left parts of the plane ($\beta \geq 0.5$) one needs $\delta Z_p/Z_p \leq 0.1\%$ to get 10% accurate C_f . Gray lines in Fig. 8 (for clarity only shown for a subset of the colored squares) indicate the range within which at least $2/3$ of the actually fitted β_f and Δ_f lie. The range is larger for Δ (horizontal lines) than for β (vertical lines). This is plausible from Fig. 4, from the area confined by multiple Z_p curves. Repeating Fig. 8 but demanding 10% accuracy for Δ_f instead of C_f yields a similar pattern in the β - Δ -plane (not shown), while demanding 10% accuracy for β_f gives a much more homogeneous pattern (0.2% to 0.5% accuracy for \tilde{Z}_p , not shown).

For highly compressible turbulence, best-fit β_f and Δ_f are expected to lie in the lower part of the β - Δ -plane in Fig. 8, roughly $\beta \leq 1/3$ and $\Delta \geq 2/3$ (Boldyrev 2002; Padoan et al. 2004; Pan et al. 2009). Here, accuracies of 0.5%, 0.1%, and 0.05% for the \tilde{Z}_p translate into accuracies of 10%, 2%, and 1% for β_f and Δ_f (not shown). Fits of similar quality require much more accurate \tilde{Z}_p in the mildly compressible regime, where $\beta > 1/3$ (upper part of panels in Fig. 8) and ultimately $\beta = 2/3$ in the incompressible limit. We note that in practical applications, best-fit values may be further improved by combining, for example, data from different time slices (Pan et al. 2009).

In summary, a 2% (1%) accurate simultaneous fit for β_f and Δ_f should be possible in the highly compressible regime if the Z_p are 0.1% (0.05%) accurate. If no satisfying fit is possible for such Z_p , this may indicate that the model is not applicable to the turbulence data under examination.

3. Discussion

We address three topics. First, can the necessary accuracy for the Z_p be met in practical applications? Second, if we had this type of accurate simulation data, what could be learned about the hierarchical structure model and its applicability or non-applicability to driven, isothermal, supersonic turbulence in a 3D periodic box? Third, we want to briefly revisit the frequently used one parameter fits.

We start with the question whether 0.1% or even 0.05% accurate Z_p for $p = 1, \dots, 5$ are achievable, as are needed to

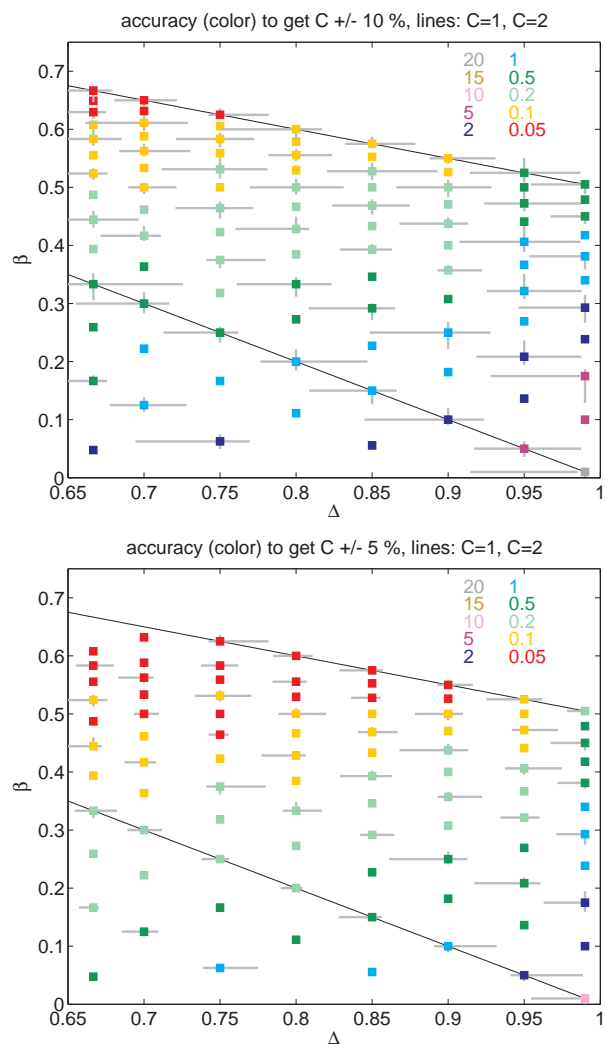


Fig. 8. Required accuracy (color coding) of perturbed Z_p , $p = 1, \dots, 5$, such that for at least $2/3$ of the best-fit pairs (β_f, Δ_f) the associated C_f are within 10% (top) or 5% (bottom) of the C associated with the initial, unperturbed (β, Δ) pair. As can be seen, the required accuracy depends crucially on the location within the β - Δ plane. Gray lines indicate the range within which $2/3$ of the actual β_f (vertical direction) and Δ_f (horizontal direction) lie. Black lines indicate constant $C = 1$ (lower line) and $C = 2$ (upper line). For details see text.

get 2% (1%) accurate fits for β and Δ . The answer is probably yes, at least in the context of 3D periodic box simulations. Schmidt et al. (2008) estimate the accuracy of their Z_p , $p = 1, \dots, 5$, to 1% (3D box simulations, 1024^3). Kritsuk et al. (2007a) estimate 1% accuracy or better for absolute scaling exponents ζ_p , $p = 1, \dots, 3$ (3D box simulations, 1024^3). Meanwhile, 3D box simulations with 4096^3 exist (e.g. Federrath 2013; Beresnyak 2014). A first order estimate suggests the four times better resolution to translate into four times (first order scheme) or 16 times (second order scheme) more accurate structure functions, thus accuracies of 0.25% or even 0.0625%. Moreover, if the accuracy of the Z_p is good enough to avoid double peaked histograms as in Fig. 6, accuracy may be further enhanced by exploring multiple time slices. Pan et al. (2009) (3D box simulations, 1024^3) used data from nine time slices for their two parameter fit. Their work is comparable although they rely on dissipation rates instead of velocity structure functions, since the involved scaling exponents (τ_p for the dissipation rate) are struc-

turally similar according to Kolmogorov's refined similarity hypothesis (Kolmogorov 1962), $\zeta_p = p/3 + \tau_{p/3}$. The tests we carried out using ratios of τ_p instead of ζ_p indeed show a similar behavior. From the quality of their fit and based on our results, we estimate their τ_p to be about 1% accurate, which is plausible given their numerical resolution. A reliable two parameter fit to 3D periodic box data of highly supersonic turbulence that is based on velocity structure functions thus appears feasible with today's data.

What could be learned from better simulation data (4096³ or better) and associated, more accurate Z_p ? Each Z_p defines a curve with associated uncertainty in the β - Δ plane, the curves for different p may or may not intersect to within uncertainties. If they intersect, the model by She & Leveque (1994) may indeed carry over to highly compressible turbulence. It is then interesting to see whether the fitted range for Δ , currently estimated as (0.67 – 0.78) by Pan et al. (2009), remains compatible with $\Delta = 2/3$, the value tacitly assumed in a large body of literature. It is also interesting to check whether $\beta = 1/3$, as theoretically anticipated by Boldyrev (2002). If indeed $(\beta, \Delta) = (1/3, 2/3)$, results from one parameter fits that quantify the transition to incompressible turbulence ($\beta = \Delta = 2/3$) with decreasing Mach number likely apply (Padoan et al. 2004). If $\Delta \neq 2/3$, two parameter fits for β and Δ would also be needed in the mildly compressible regime. However, the analysis in Sect. 2.3.3 suggests that these kind of fits are likely beyond reach of today's computer resources.

The latter of the above cases, where the Z_p curves do not intersect to within their uncertainty, would imply that the model by She & Leveque (1994) does not carry over to 3D periodic box simulations of driven, isothermal, highly compressible turbulence. A simple reason here could be that theoretical results are based on the assumption of an infinite Reynolds number, a criterion clearly violated by numerical simulations. More importantly, She & Waymire (1995) already pointed out that there is no reason why only one dimension should be associated with the most dissipative structure. They argued that in such a large portion of space as is typically analyzed, a variety of most dissipative structures may co-exist with different co-dimensions. Hopkins (2013) suggests a slightly different model based on work by Castaing (1996), which is more compatible with not strictly log-normal density PDFs as observed in isothermal supersonic turbulence. Finally, yet other models exist, (e.g. via multifractals Macek et al. 2011; Zybin & Sirota 2013), as well as other perspectives on the fractal character of a turbulent medium (see e.g. Kritsuk et al. 2007a).

Lastly, we briefly come back to the one parameter fits that are often used in the literature. Fixing the value of Δ by hand greatly reduces the impact of uncertainties in the Z_p on the accuracy of the estimated best-fit co-dimension C_f . Folini et al. (2014) found 5% uncertain Z_p , $p = 1, \dots, 5$, to translate into roughly 10% uncertainty of the C_f for fixed $\Delta = 2/3$. Fig. 3 offers a qualitative understanding of this reduced "error propagation", which suggests some sensitivity to the specific location in the β - Δ -plane, and indicates that fixing C or β instead of Δ has a similar effect. Fixing β seems questionable at first sight since there is, to our knowledge, little theoretical understanding of what numerical value β might have (see e.g. Dubrulle 1994). On the other hand, She et al. (2001) presented a theoretical framework that allows for an independent determination of only β from the relative scaling exponents Z_p (see also Hily-Blant et al. (2008), their Appendix A3). One could thus imagine breaking the two parameter fit for β and Δ into a two step procedure: first, fix the value of β , then use this value and do a one parameter fit for Δ . Hopefully

this type of a two step approach is more robust against uncertainties in the Z_p , but this question is beyond the scope of the current paper and we are unaware of corresponding attempts in the literature.

4. Summary and conclusions

This study was motivated by the overarching question of whether or not the random cascade model (She & Leveque 1994; Dubrulle 1994; She & Waymire 1995; Boldyrev 2002) applies to simulation data of highly compressible isothermal turbulence and, if so, with what parameter values for β and Δ . If applicable, the model offers a theoretical link between observable properties of the turbulence, namely ratios Z_p of scaling exponents of the structure functions, and non-observable turbulence characteristics, for example the dimension D of the most dissipative structures. To date, applicability of the model is assumed in much of the literature with $\Delta = 2/3$, a value just marginally compatible with simulation-based best estimates (Pan et al. 2009): $\Delta = 0.71$ with an uncertainty range $\Delta \in (0.67, 0.78)$.

We examine how uncertainties in the Z_p translate into uncertainties of best-fit β - Δ -pairs and discuss what best-fits, consequently, seem achievable with today's computer resources. A Monte Carlo approach is used to mimic actual simulation data. The results can be summarized in six main points.

- Simultaneous fitting of β and Δ to sets of substantially (5%) perturbed (uncertain) Z_p yields a "double peaked ridge" of best-fit values in the β - Δ plane. None of the two peaks is co-located with the initial (β, Δ) pair.
- The highest and lowest order p are particularly relevant for simultaneous fitting of β and Δ . A somewhat optimal choice is $p = 1, \dots, 5$. Yet higher order structure functions add comparatively little to the quality of the fit, while they tend to be afflicted with larger uncertainties in real applications.
- A simultaneous, 2% (1%) accurate fit of β and Δ should be possible if the Z_p , $p = 1, \dots, 5$, are 0.1% (0.05%) accurate and if the (yet to be determined) value of β is about 1/3 or less.
- Applicability of the model thus may be best tested in the highly compressible regime, where $\beta \approx 1/3$ is expected, and not in the mildly compressible regime where β ultimately must approach its incompressible value of 2/3.
- We argue that today's computer resources likely allow to reach this accuracy. Existing simulations of 4096³ (Federrath 2013; Beresnyak 2014) probably allow for at least 2%, possibly 1% accurate estimates of β and Δ .
- Should the ambiguity in the determination of β and Δ persist despite such highly accurate Z_p , this may indicate that the notion of She & Waymire (1995) (β and Δ take a continuum of values) or Hopkins (2013) (a different model for the statistics of the inertial range) is correct or that yet a different turbulence model is needed in this regime.

While the authors lack the computational resources to really test the estimates presented here, this study may encourage other groups to analyze their data in the light of this study.

Acknowledgements. RW and DF acknowledge support from the French National Program for High Energies PNHE. We acknowledge support from the Pôle Scientifique de Modélisation Numérique (PSMN), from the Grand Equipement National de Calcul Intensif (GENCI), project number x2014046960, and from the European Research Council through grant ERC-AdG No. 320478-TOFU.

References

- Benzi, R., Ciliberto, S., Tripicciono, R., Baudet, C., Massaioli, F., & Succi, S. 1993, *Phys. Rev. E*, 48, 29
- Beresnyak, A. 2014, *ApJ*, 784, L20
- Boldyrev, S. 2002, *ApJ*, 569, 841
- Boldyrev, S., Nordlund, Å., & Padoan, P. 2002, *Phys. Rev. Letters*, 89, 031102
- Castaing, B. 1996, *Journal de Physique II*, 6, 105
- Chabrier, G. & Hennebelle, P. 2011, *A&A*, 534, A106
- Dobler, W., Haugen, N. E., Yousef, T. A., & Brandenburg, A. 2003, *Phys.Rev.E*, 68, 026304
- Dubrulle, B. 1994, *Phys. Rev. Letters*, 73, 959
- Federrath, C. 2013, *MNRAS*, 436, 1245
- Federrath, C. & Klessen, R. S. 2012, *ApJ*, 761, 156
- Folini, D., Walder, R., & Favre, J. M. 2014, *A&A*, 562, A112
- Gustafsson, M., Brandenburg, A., Lemaire, J. L., & Field, D. 2006, *A&A*, 454, 815
- Hennebelle, P. & Chabrier, G. 2008, *ApJ*, 684, 395
- Hily-Blant, P., Falgarone, E., & Pety, J. 2008, *A&A*, 481, 367
- Hobbs, A., Nayakshin, S., Power, C., & King, A. 2011, *MNRAS*, 413, 2633
- Hopkins, P. F. 2013, *MNRAS*, 430, 1880
- Kolmogorov, A. N. 1962, *Journal of Fluid Mechanics*, 13, 82
- Kritsuk, A. G., Lee, C. T., & Norman, M. L. 2013, *MNRAS*, 436, 3247
- Kritsuk, A. G., Norman, M. L., Padoan, P., & Wagner, R. 2007a, *ApJ*, 665, 416
- Kritsuk, A. G., Padoan, P., Wagner, R., & Norman, M. L. 2007b, in *American Institute of Physics Conference Series*, Vol. 932, *Turbulence and Nonlinear Processes in Astrophysical Plasmas*, ed. D. Shaikh & G. P. Zank, 393–399
- Lazar, A., Nakar, E., & Piran, T. 2009, *ApJ*, 695, L10
- Le Maître, O. P. & Knio, O. M. 2010, *Spectral Methods for Uncertainty Quantification* (Springer)
- Macek, W. M., Wawrzaszek, A., & Carbone, V. 2011, *Geophys. Res. Lett.*, 38, 19103
- Najm, H. N. 2009, *Annual Review of Fluid Mechanics*, 41, 35
- Narayan, R. & Kumar, P. 2009, *MNRAS*, 394, L117
- Padoan, P., Haugbølle, T., & Nordlund, Å. 2012, *ApJ*, 759, L27
- Padoan, P., Jimenez, R., Nordlund, Å., & Boldyrev, S. 2004, *Phys. Rev. Lett.*, 92, 191102
- Pan, L., Padoan, P., & Kritsuk, A. G. 2009, *Physical Review Letters*, 102, 034501
- Schmidt, W., Federrath, C., Hupp, M., Kern, S., & Niemeyer, J. C. 2009, *A&A*, 494, 127
- Schmidt, W., Federrath, C., & Klessen, R. 2008, *Phys. Rev. Lett.*, 101, 194505
- She, Z.-S. & Leveque, E. 1994, *Phys. Rev. Lett.*, 72, 336
- She, Z.-S., Ren, K., Lewis, G. S., & Swinney, H. L. 2001, *Phys. Rev. E*, 64, 016308
- She, Z.-S. & Waymire, E. C. 1995, *Phys. Rev. Letters*, 74, 262
- She, Z.-S. & Zhang, Z.-X. 2009, *Acta Mechanica Sinica*, 25, 279
- Walder, R., Folini, D., & Shore, S. N. 2008, *A&A*, 484, L9
- Zybin, K. P. & Sirota, V. A. 2013, *Phys. Rev. E*, 88, 043017